Statistical estimation of trailing edge noise from finite wall-mounted airfoils

Jesse Coombs[1], Con Doolan[2], Anthony Zander[1], Danielle Moreau[2] and Laura Brooks[3]

[1] School of Mechanical Engineering, University of Adelaide, Adelaide, South Australia, 5005, Australia
[2] School of Mechanical and Manufacturing Engineering, UNSW, Sydney, NSW, 2052, Australia
[3] ASC Pty Ltd, Osborne, South Australia, 5017, Australia

ABSTRACT

It is important to be able to accurately model the flow and noise generated by finite wall-mounted airfoil flows because of the many engineering applications in which these flows occur. One method for predicting turbulent trailing edge noise is the Reynolds-averaged Navier-Stokes based statistical noise model (RSNM) of Doolan et al. (*Proceedings of 20th International Congress on Acoustics*, ICA 2010). The RSNM method has previously been used successfully on a range of two-dimensional geometry-flow cases. In this paper a new turbulent velocity cross-spectrum model and improved implementation are proposed to allow the RSNM method to be used to effectively and efficiently predict turbulent trailing edge noise from more complex three-dimensional cases. Reynolds-averaged Navier-Stokes (RANS) simulations of a series of wing-in-junction cases are used in combination with the developed acoustic model to predict the far-field noise and compared against experimental noise measurements.

1. INTRODUCTION

Finite wall-mounted airfoil flows occur where wing-like shapes are attached to a fuselage or hull. The noise generated by finite wall-mounted airfoil flows has a number of significant impacts. In the aviation industry, noise is a health concern for those that live and work near airfields (Bronzaft et al., 1998; Kaltenbach et al., 2008). In the maritime industry, reduction of noise for stealth is an especially important consideration for military designs (Defence Science and Technology Organisation, 2004). In these applications and elsewhere, it is important to be able to accurately model the flow and noise generated by wing-in-junction flows.

Finite wall-mounted airfoil flows exhibit a number of noise production mechanisms, including turbulent boundary layer noise, leading edge noise, turbulent boundary layer trailing edge noise (TBL-TE), and tip noise. For noise modelling to be part of the engineering design process, methods of predicting the noise resulting from these mechanisms must be accurate and efficient. This paper aims to extend the RANS-based statistical noise model (RSNM) (Doolan et al., 2010) to three-dimensions, to apply the extension to a series of wing-in-junction test cases, and to compare the resulting predicted noise to experimental anechoic wind tunnel measurements.

2. METHODOLOGY

2.1 RANS-based Statistical Noise Model (RSNM)

The RANS-based Statistical Noise Model (RSNM) developed by Doolan et al. (2010) can be used to predict TBL-TE noise. Based on the theory of Ffowcs-Williams and Hall (1970) the method calculates the sound intensity in the far field created by turbulent flow past a sharp trailing edge by means of a Green's function approach. The Green's function appropriate for the sharp, straight trailing edge of an airfoil is a rigid half plane Green's function (Albarracin et al., 2012). The resulting far field pressure fluctuations are obtained by convolution of the source terms with the Green's function. These source terms are obtained from mean flow data, typically taken from a RANS-based simulation, by means of a two-point space-time-correlation function model of the form (Morris and Farassat, 2002)

$$R_m(\mathbf{y_1},\boldsymbol{\eta},\tau)=Au_s^2 \exp\left(-\frac{|\boldsymbol{\eta}|^2}{l_s^2}-\omega_s^2\tau^2\right) \quad (1)$$

where $\mathbf{y_1}$ is the position of the first point, $\boldsymbol{\eta}$ the separation between the two points ($\boldsymbol{\eta}=\mathbf{y_2}-\mathbf{y_1}$), A is an empirical scalar value that determines the magnitude of the correlation, l_s the characteristic length scale of the flow, ω_s is a characteristic frequency, u_s is a velocity scale that characterises the velocity fluctuations, and τ the correlation time

delay.

Using this two point model (Albarracin et al., 2012) the turbulent velocity cross-spectrum becomes in the frequency (ω) domain

$$\Phi(\mathbf{y_1},\boldsymbol{\eta},\omega) = \frac{\mathrm{Au_s^2}\sqrt{\pi}}{\omega_s}\exp\left(-\frac{|\boldsymbol{\eta}|^2}{l_s^2}\right)\exp\left(-\frac{\omega^2}{4\omega_s^2}\right) \quad (2)$$

where the model is tied to the RANS turbulence properties by

$$u_s=\sqrt{\frac{2k}{3}},\ \omega_s=\frac{2\pi}{\tau_s},\ \tau_s=\frac{c_\tau k}{\epsilon},\ l_s=\frac{c_l k^{\frac{3}{2}}}{\epsilon} \quad (3)$$

where k and ϵ are the RANS solution turbulent kinetic energy and turbulent dissipation, respectively, and where c_τ and c_l are semi-empirical parameters.

RSNM as originally proposed (Albarracin et al., 2012) evaluates the far-field power spectral density $S(x,\omega)$, given analytically as a double integral, numerically by means of a double summation, in terms of volume V as

$$S(x,\omega) \propto \sum_{V(y_1)}\sum_{V(y_2)}\Phi(\mathbf{y_1},\boldsymbol{\eta},\omega)\,\mathrm{d}V(y_1)\mathrm{d}V(y_2) \quad (4)$$

To date the RSNM method has been used successfully on a range of two-dimensional geometry-flow cases including sharp edged flat plates and various airfoils (Doolan et al., 2010, Albarracin et al., 2012, Marshallsay et al. 2013). In many of these cases, the spanwise extent was accounted for by means of a correction factor following the approach of Corcos (1964). However, such a correction would not be suitable for application to more complex three-dimensional cases. Furthermore, to achieve accurate evaluation of the far-field power spectral density using such an implementation requires the volumes considered to have extents smaller than the characteristic length scales l_s. The fine spatial discretisation required to meet this criteria, especially for three-dimensional flow cases, can be prohibitively computationally intensive. These limitations drove the desire to develop a new turbulent velocity cross-spectrum which would take into account the spanwise extent implicitly, as well as an improved implementation which would allow for larger volumes, drastically reducing the complexity of the resulting noise calculation.

2.2 3D RSNM Methodology And Expectation Value Implementation

To extend the application of the RSNM method to three-dimensional cases, the following adaptation to the previously detailed turbulent velocity cross-spectrum is proposed:

$$\Phi(\mathbf{y_1},\eta,\omega) = \frac{\mathrm{Au_s^2}\sqrt{\pi}}{\omega_s}\phi_x\phi_y\phi_z\phi_\omega \quad (5)$$

where $\phi_\omega = \exp\left(-\frac{\omega^2}{4\omega_s^2}\right)$, and $\phi_i = \exp\left(-\frac{|\boldsymbol{\eta_i}|^2}{l_{s_i}}\right)$ are orthogonal x, y and z separation and lengthscale components. Such a form allows for differing correlation lengths to be applied to each direction. In the present study, x and y lengthscale constants are set to take the same values as in the work of Albarracin (2012), namely by setting $c_{l_x} = c_{l_y}$ = 0.012U_{ref} + 0.73, where U_{ref} is the freestream flow velocity, and $c_{l_z} = 5$, which was found to produce good agreement with the experimental data.

The originally proposed implementation has the downside that, by treating the cross-spectrum as a point property when evaluating the cross-spectrum in instances where $y_1 = y_2$, regardless of the physical extent of the volume ($V(y_1)$), it is assumed to produce noise as though completely correlated with itself ($\boldsymbol{\Phi(\mathrm{y}_1,0,\omega)} = 1$). This a reasonable assumption provided the extent of the volume in question is less than the characteristic length scale, however, if the extent of the cell is greater than the characteristic length scale, then the originally proposed implementation will result in an overestimation of the resulting far-field power spectral density. It would be impractical in most anticipated applications of the method to have spanwise spatial discretisation with resolution approximately the same or smaller than the characteristic lengthscale, as it would significantly increase both the

computational effort of the CFD needed as an input and the subsequent noise calculation. In order to combat this overestimation to more accurate calculate the far-field power spectral density, as well as to allow volumes of arbitrary extent, instead of the expression given by Equation 4, the following implementation is proposed:

$$S(x,\omega) \propto \sum_{V(y_1)} \sum_{V(y_2)} <\Phi(\mathbf{y_1},\boldsymbol{\eta}^*,\omega)> \mathrm{dV}(y_1)\mathrm{dV}(y_2) \tag{6}$$

where $<\Phi(\mathbf{y_1},\boldsymbol{\eta}^*,\omega)>$ is the expectation value for the velocity cross-spectrum based on average separation of points ($\boldsymbol{\eta}^*$) within the respective volumes. Recalling that the separation components are independent,

$$< \Phi(\mathrm{y}_1,\eta^*,\omega) >= \frac{\mathrm{Au}_s^2\sqrt{\pi}}{\omega_s} < \phi_x >< \phi_y >< \phi_z >< \phi_\omega > \tag{7}$$

and that the frequency component has no separation dependence so,

$$< \phi_\omega >= \phi_\omega \tag{8}$$

whereupon only an expression for $< \phi_i >$ is required. In order to develop such an expression, consider a cell of extent $[0, L]$ in the x direction, with a point at the cell centre $\mathrm{x}_1 = \frac{L}{2}$ and point x_2 located randomly over the x-direction extent of the cell. This means that probability density function of point x_2 is given by

$$f_{x_2} = \frac{1}{L}, z \in [0, L] \text{ else } f_{x_2} = 0 \tag{9}$$

Hence

$$< \phi_x > = \int_{-\infty}^{\infty} \phi_x(\mathrm{x}_2) f_{x_2} dx_2 = \int_0^L \exp\left(-\frac{\left|\frac{L}{2} - x_2\right|^2}{l_{s_x}} \right) \frac{1}{L} dx_2 \tag{10}$$

reduces to

$$< \phi_x >= \frac{l_{s_x}}{L} \times \mathrm{erf}(\frac{L}{2\, l_{s_x}}) \tag{11}$$

where erf is the error function (also known as the Gauss error function). The same arguments may be used to develop expressions for $< \phi_y >$ and $< \phi_z >$.

3. TEST CASE AND RANS SIMULATIONS

The proposed model and implementation are applied to a series of test cases following the experiments of Moreau et al. (2016), in which acoustic beamforming was used to investigate the noise from finite wall-mounted airfoils. Moreau et al. (2016) obtained took acoustic measurements for a series of wall-mounted NACA 0012 profile airfoils with tripped turbulent boundary layers, which all had flat-ended tips and for a range of span (S) to chord (C) aspect ratios (AR) of S/C = AR = [1,3], chord based Reynolds numbers $Re_c = [8 \times 10^5, 1.6 \times 10^6]$, and geometric angles of attack AOA $= [0,12]$ degrees. The present work will investigate the same aspect ratios, and some of the angles of attack as Moreau et al. (2016), but at only the highest Reynolds number, and with the simplifying assumption of a sharp trailing edge.

The mean flow data required for the noise calculation were obtained by means of steady state RANS simulation, using the semi-implicit method for pressure-linked equations (SIMPLE) algorithm (Ferziger and Peric 1999). RANS closure was achieved using the k-ω SST turbulence model (Menter 1992), while the flow calculations were run using OpenFOAM (Weller et al., 1998). The computational domains, shown diagrammatically in Figure 1, had a half-width of 3 C, extended 10 C downstream of the wing and 5.1 C upstream, a distance set so as to develop a boundary layer approaching the wing to match that measured experimentally by Moreau et al. (2016). The top

computational boundary is set so as to be 10 S from the bottom boundary. The meshes used have a structured CH topology near the wing, as well as a structured far-field region, with a connecting unstructured region, as shown in Figure 2.

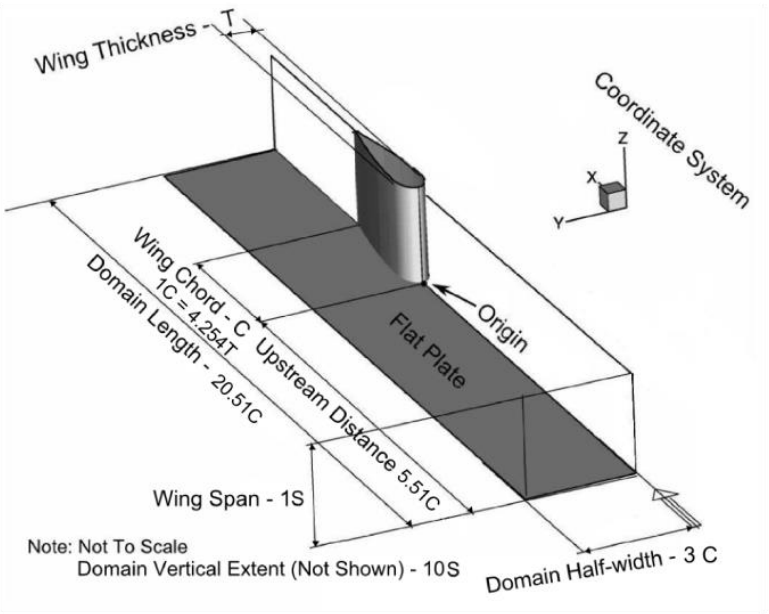

Figure 1: Case geometry and computational domain diagram

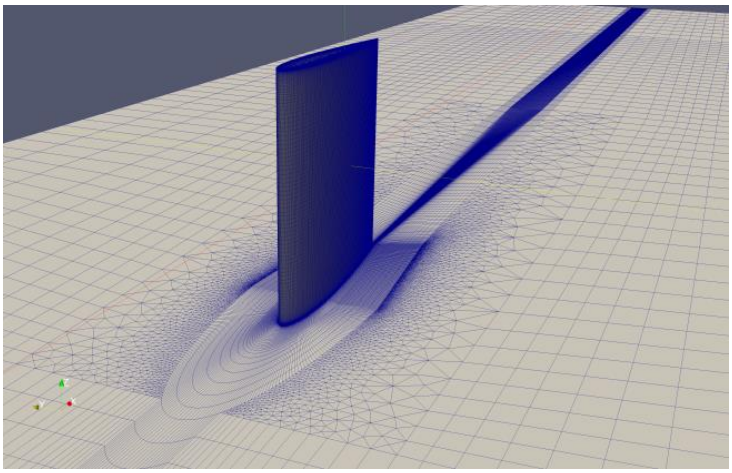

Figure 2: Mesh geometry diagram

4. RESULTS AND DISCUSSION

4.1 Flow Results

Although providing extensive acoustic results, the flow results of Moreau et al. (2016) are somewhat more limited. Hence flow comparisons will be made to the more extensive flow results of Giuni and Green (2013). Who obtained flow measurements of a flat ended NACA0012 airfoil at the marginally reduced chord based Reynolds number of 740,000. Giuni and Green (2013) obtained measurements of axial velocity and vorticity in a plane one quarter chord length downstream of the wing trailing edge. Results for the AR = 1, AOA = 0 degrees case of Giuni and Green (2013), are compared with those of the present study for the same aspect ratio and angle of attack, in Figures 3 and 4 respectively. The axial velocities are normalised by freesteam flow speed, distances are given in chord normalised units, and the vorticities are given normalised by freesteam flow velocity and chord. Results from the present work are presented in a coordinate system that is otherwise the same as that of Giuni and Green

(2013), which has origin at the wing tip trailing edge, except for the y-axis having the opposite sense so as to preserve the right handedness of the coordinate system. The low axial velocity regions of the present work and that of Giuni and Green (2013) have the same structure, although it can be seen that larger and more intense low flow regions are observed in the present work.

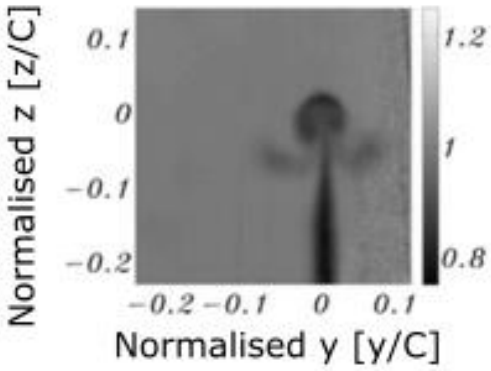

(a) Adapted from Giuni and Green (2013)

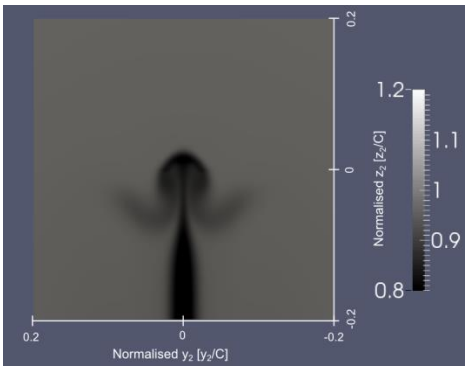

(b) Present work

Figure 3: Near wake normalized axial velocity comparison

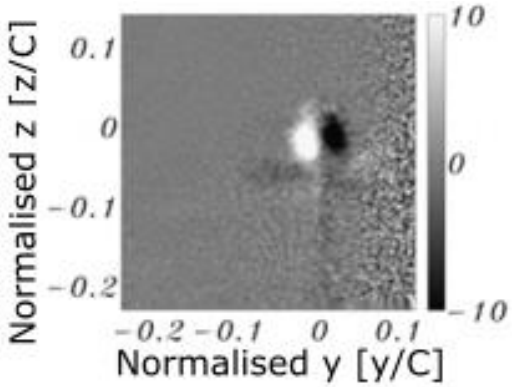

(a) Adapted from Giuni and Green (2013)

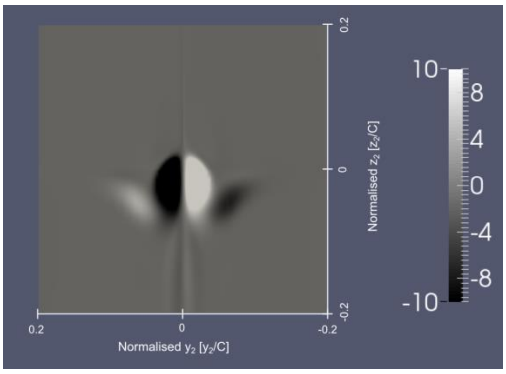

(b) Present work

Figure 4: Near wake normalized x-plane vorticity comparison

4.2 Acoustic Results

Flow data were extracted from the RANS modelling over a region centred on the mid-span trailing edge and which extends the entirety of the airfoil span, as well as one trailing edge boundary layer thickness length upstream, down-stream and across-stream. A sample region of this extent has proven sufficient in previous studies (Doolan et al., 2010, Albarracin et al., 2012, Marshallsay et al. 2013). Data from this region was used to estimate the turbulent boundary layer trailing edge noise using the 3D RSNM methodology and expectation value implementation.

Noise predictions are compared to the total noise measurements, as well as the isolated trailing edge noise components as determined by means of integrating the sound maps over the trailing edge region of Moreau et al. (2016) in Figures 5 to 13. Good agreement is generally found between the modelled and measured trailing edge noise except at the lowest frequencies (<1kHz), where the model underpredicts the levels of Moreau et al. (2016). The sound maps of Moreau et al. (2016) reveal that as the frequency decreases, the strongest noise sources transition from the tip trailing edge and the entire span of the trailing edge, to the wing-junction mid chord. This suggests that at the lowest frequencies considered, turbulent boundary layer trailing edge noise is no longer the dominant noise mechanism, and so it is unsurprising that a trailing edge noise model underpredicts the total noise in such conditions. The model also does not capture the peak which occurs between 3 and 4 kHz for the cases at 6 and 12 degrees angle of attack, which is attributed to the dominant tip noise, nor the peak at approximately 2kHz which is attributed to TE bluntness vortex shedding, and which was not replicated by the simulated sharp edged airfoils. The traditional explanation of tip noise is an enhancement in turbulent trailing-edge noise caused by increased turbulence about the tip region due to the tip vortices (George and Chou 1984). However, in the highest reported frequency sound map of Moreau et al. (2016) where tip noise is dominant, there are sources near both the leading and trailing edges. These observations are not consistent with the George and Chou (1984) explanation, and additional mechanisms or a more complex model may be required for a complete description of tip noise.

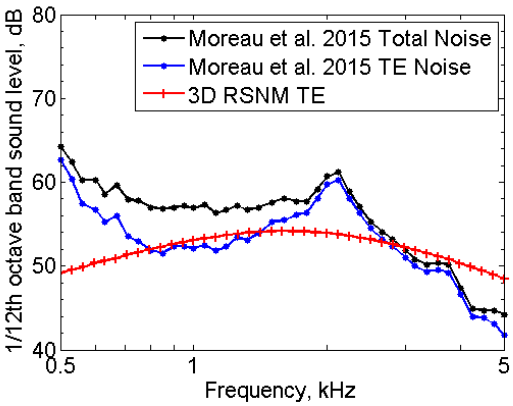

Figure 5: AR=1, AOA=0 degrees case noise prediction and comparison to results of Moreau et al. (2016)

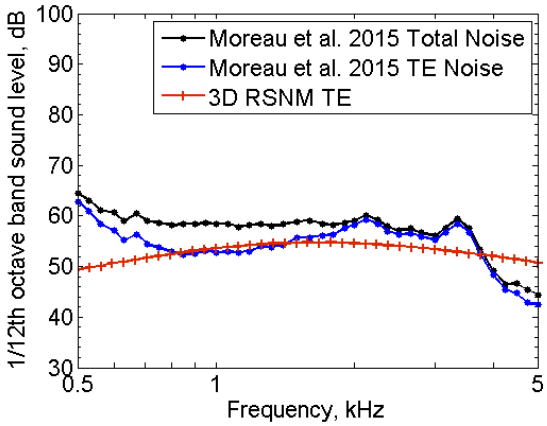

Figure 6: AR=1, AOA=6 degrees case noise prediction and comparison to results of Moreau et al. (2016)

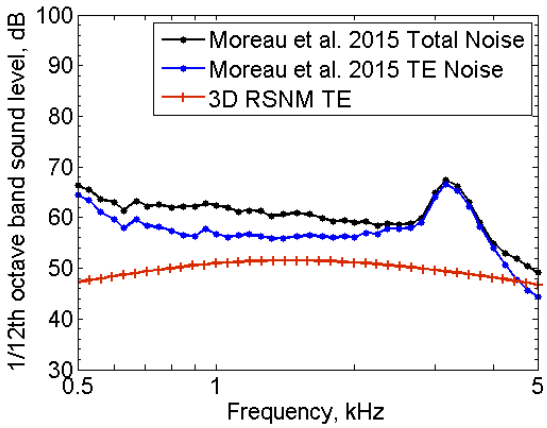

Figure 7: AR=1, AOA=12 degrees case noise prediction and comparison to results of Moreau et al. (2016)

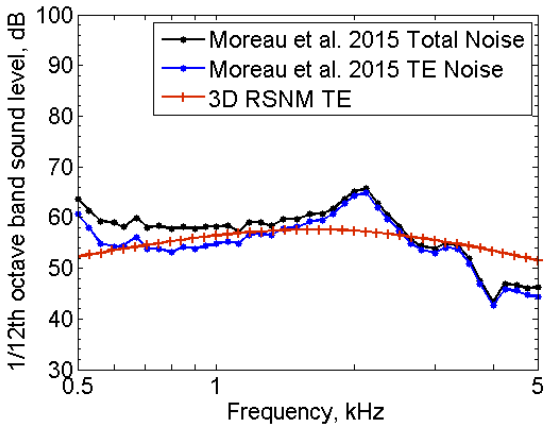

Figure 8: AR=2, AOA=0 degrees case noise prediction and comparison to results of Moreau et al. (2016)

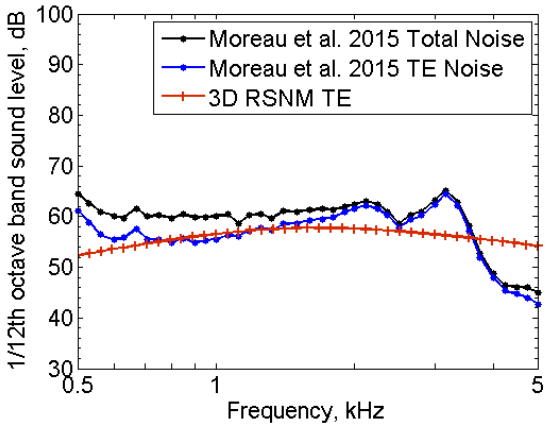

Figure 9: AR=2, AOA=6 degrees case noise prediction and comparison to results of Moreau et al. (2016)

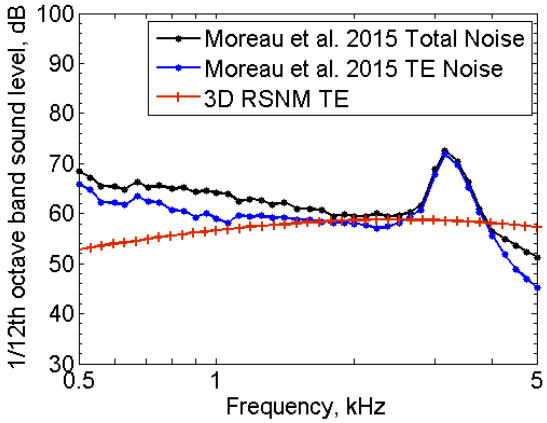

Figure 10: AR=2, AOA=12 degrees case noise prediction and comparison to results of Moreau et al. (2016)

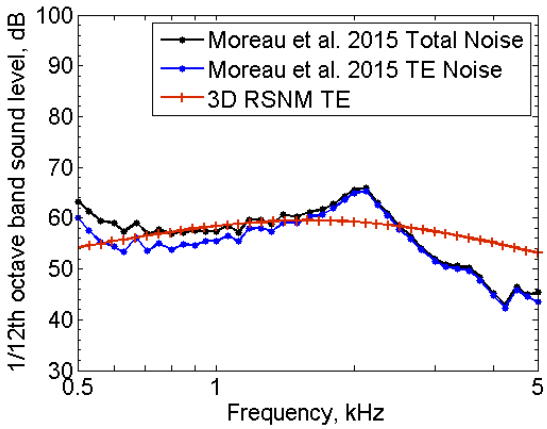

Figure 11: AR=3, AOA=0 degrees case noise prediction and comparison to results of Moreau et al. (2016)

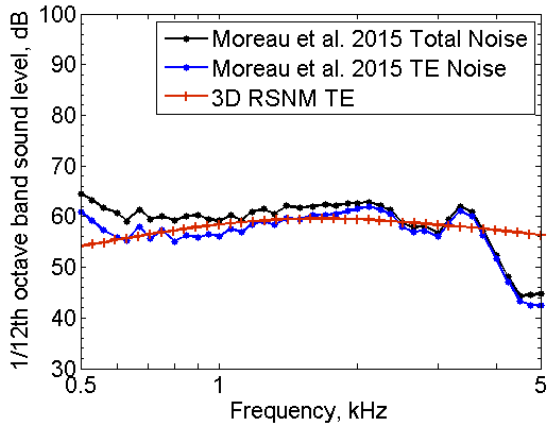

Figure 12: AR=3, AOA=6 degrees case noise prediction and comparison to results of Moreau et al. (2016)

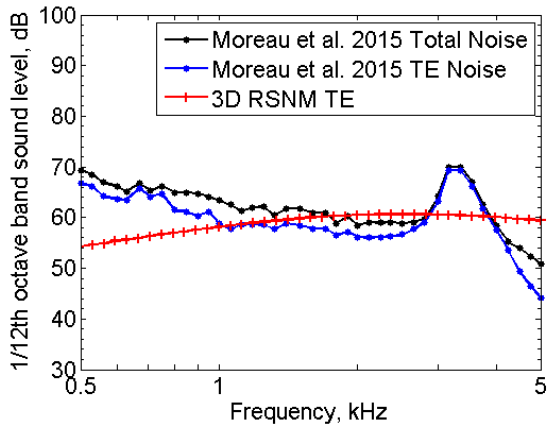

Figure 13: AR=3, AOA=12 degrees case noise prediction and comparison to results of Moreau et al. (2016)

5. CONCLUSIONS

The RANS-based Statistical Noise Model was extended so as to be suitable for applications involving spanwise variations in wing geometry or flow properties. An improved implementation was proposed which more accurately predicts the average correlation within a cell, and which should also reduce the grid dependence of the noise prediction as well as allow for larger cell volumes to be considered. The proposed model and implementation were applied to predict the noise from a series of finite wall-mounted airfoil flow cases from the recent literature. Generally good agreement was found between the predicted and experimentally measured noise levels for frequencies where trailing edge noise dominates. At frequencies where other noise mechanisms were dominant, such as at the lowest frequencies, the modelled noise underpredicts that of the experiment. The proposed model is expected to be of interest, as it allows for predictions for more complex wing-flow conditions that are likely more representative of practical applications. The improved implementation is also of benefit, due to it reducing the dependence on the spatial discretisation and thereby reducing the computational intensity of the noise calculation through reduction in the number of cells required for effective spatial discretisation.

ACKNOWLEDGEMENTS

The Authors would like to acknowledge the many helpful discussions with Mr. Cristobal Albarracin regarding the RSNM method and its implementation.

REFERENCES

Albarracin, C, Doolan, C, Jones, R, Hansen, C, Brooks, L & Teubner, M 2012, 'A RANS-based Statistical Noise Model for Trailing Edge Noise', *AIAA 18th AIAA/CEAS Aeroacoustics Conference*, Colorado Springs, USA.

Bronzaft, A, Ahern, K, McGinn, R, O'Connor, J & Savino, B 1998, 'Aircraft noise: A potential health hazard.' *Environment and Behavior*, volume 30, pp. 101-113.

Corcos, G 1964, 'The structure of the turbulent pressure field in boundary-layer flows', *Journal of Fluid Mechanics*, Vol. 18, No. 3, pp. 353-378.

Defence Science and Technology Organisation 2004, 'Some aspects of submarine design part 1. Hydrodynamics', Technical report.

Doolan, C, Gonzalez, C & Hansen, C 2010, 'Statistical estimation of turbulent trailing edge noise.', *Proceedings of 20th International Congress on Acoustics*, ICA.

Ffowcs-Williams, J & Hall, L 1970, 'Aerodynamic sound generation by turbulent flow in the vicinity of a scattering half plane', *Journal of Fluid Mechanics*, vol. 40, pp. 657-670.

Ferziger, J and Peric, M 1995, *Computational methods for fluid dynamics*. Springer-Verlag.

George, A & Chou, T-S 1984, *Broadband rotor noise analyses*. Vol. 3797. National Aeronautics and Space Administration, Scientific and Technical Information Office.

Giuni, M and Green, R 2013, 'Vortex formation on squared and rounded tip.' *Aerospace Science*, Vol 29(1), pp. 191-199.

Kaltenbach, M, Maschke, C & Klinke, R 2008, 'Health consequences of aircraft noise.' Deutsches Arzteblatt International, volume 105, pp. 548–556.

Marshallsay, P, Brooks, L, Cederholm, A, Doolan, C, Moreau, D & Albarracin, C 2013, 'Improved Delayed Detached Eddy Simulation modeling and far-field trailing-edge noise estimation of a sharp-edged symmetric strut.', *Proceedings of Meetings on Acoustics*, Vol. 19. No. 1. Acoustical Society of America.

Menter, F 1992, 'Improved two-equation k-ω turbulence models for aerodynamic flows NASA Ames, CA' *NASA Technical Memorandum TM-103975*.

Moreau, D, Doolan, C, Alexander, W, Meyers, T, & Devenport, W 2016, 'Wall-Mounted Finite Airfoil Noise Production and Prediction.' *AIAA*, Vol. 54(5), pp. 1637–1651.

Morris P & Farassat F 2002, 'Acoustic Analogy and Alternative Theories for Jet Noise Prediction.', *Proceedings of AIAA*, Vol. 40(5), pp. 671-680.

Weller, H, Tabor G, Jasak, H & Fureby, C 1998, 'A tensorial approach to CFD using object oriented techniques' *Computers in Physics*, Vol. 12, pp. 620-631.